4720 *Biochemistry* **2009,** *48,* 4720–4727
DOI: 10.1021/bi900037s

BIOCHEMISTRY
including biophysical chemistry & molecular biology
Article

Myelin Basic Protein Binds to and Inhibits the Fibrillar Assembly of Aβ42 in Vitro[†]

Michael D. Hoos,[‡] Mahiuddin Ahmed,[§] Steven O. Smith,[§] and William E. Van Nostrand*[,‡]

[‡]*Department of Medicine and* [§]*Center for Structural Biology, Stony Brook University, Stony Brook, New York 11794-8153*

Received January 9, 2009; Revised Manuscript Received April 21, 2009

ABSTRACT: The deposition of amyloid β-protein (Aβ) fibrils into plaques within the brain parenchyma and along cerebral blood vessels is a hallmark of Alzheimer's disease. Aβ peptides are produced through the successive cleavage of the Aβ precursor protein by β- and γ-secretase, producing peptides between 39 and 43 amino acids in length. The most common of these are Aβ40 (the most abundant) and Aβ42. Aβ42 is more fibrillogenic than Aβ40 and has been implicated in early Aβ plaque deposition. Our previous studies determined that myelin basic protein (MBP) was capable of inhibiting fibril formation of a highly fibrillogenic Aβ peptide containing both E22Q (Dutch) and D23N (Iowa) mutations associated with familial forms of cerebral amyloid angiopathy [Hoos, M. D., et al. (2007) *J. Biol. Chem. 282*, 9952−9961]. In this study, we show through a combination of biochemical and ultrastructural techniques that MBP is also capable of inhibiting the β-sheet fibrillar assembly of the normal Aβ42 peptide. These findings suggest that MBP may play a role in regulating the deposition of Aβ42 and thereby also may regulate the early formation of amyloid plaques in Alzheimer's disease.

Deposits of amyloid β-proteins (Aβs)[1] into plaques in the brain parenchyma and cerebrovasculature are prominent features of Alzheimer's disease (AD) and other related disorders (*1*). Aβ is derived through the sequential proteolysis of the amyloid β-precursor protein (AβPP) by β- and γ-secretase (*2*−*5*). These cleavages produce Aβ peptides between 39 and 43 amino acids in length with the most abundant being Aβ40 and Aβ42 (*6*). Aβ peptides exhibit a strong propensity to self-assemble into β-sheet-containing oligomeric forms and fibrils (*7*). It has been shown that the oligomerization and deposition of Aβ42 likely precede and, possibly, seed deposition of Aβ40 in amyloid plaques and cerebral vascular lesions, leading to neurodegeneration and dementia (*8*−*10*). Elevated levels of soluble Aβ42 have also been shown to increase the risk of developing AD pathology (*10*). For these reasons, it is important to understand the nature of Aβ42 in the CNS and how it interacts with other components of healthy and diseased brain.

Cerebral amyloid angiopathy (CAA), a condition prevalently found in AD, is characterized by fibrillar Aβ deposition within and along primarily small and medium-sized arteries and arterioles of the cerebral cortex and leptomeninges and in the cerebral microvasculature (*7*, *11*, *12*). Familial forms of CAA are caused by specific point mutations within the Aβ sequence of the AβPP gene (*13*−*18*). The most recognized example of familial CAA is the Dutch type resulting from an E22Q substitution in Aβ (*13*, *14*, *19*). Another more recently identified form of familial CAA is the Iowa-type D23N substitution in Aβ (*18*). In vitro, these familial forms of Aβ exhibit an increased propensity to form amyloid fibrils when compared to wild-type Aβ40 (Aβ40WT) (*20*−*24*). Including each of these mutations together in the same Aβ peptide (Aβ40DI) further enhances the fibrillogenic and pathogenic properties in vitro (*24*). In a recent study using a combination of biochemical assays and high-resolution microscopy techniques, we demonstrated that myelin basic protein (MBP) bound preferentially to the more fibrillogenic Aβ40DI over Aβ40WT (*25*). Furthermore, we showed that MBP effectively inhibits the fibrillar assembly of Aβ40DI. We postulated that MBP might play a role in the regulation of familial CAA mutant Aβ fibrillogenesis. However, with the improving understanding of the importance of Aβ42WT to disease processes such as AD and CAA, we examined whether MBP can act in a similar fashion on this more fibrillogenic wild-type Aβ peptide as well.

In this study, we show that MBP binds to Aβ42WT in vitro. Using a combination of biochemical assays and high-resolution microscopy, we demonstrate that MBP impedes β-sheet formation and potently inhibits Aβ42WT fibril formation. These findings lead us to postulate that endogenous MBP may play a role in regulating the fibrillar assembly and deposition of Aβ42WT in Alzheimer's disease and other related conditions.

[†]This work was supported by grants from the Alzheimer's Association (IIRG-06-26805), the Cure Alzheimer's Fund, a Collaborative MS Research Center Award, and National Institutes of Health Grant RO1-AG027317.

*To whom correspondence should be addressed: Department of Medicine, HSC T-15/083, Stony Brook University, Stony Brook, NY 11794-8153. Telephone: (631) 444-1661. Fax: (631) 444-2560. E-mail: William.VanNostrand@stonybrook.edu.

[1]Abbreviations: Aβ, amyloid β-protein; AD, Alzheimer's disease; AβPP, amyloid β-protein precursor; CAA, cerebral amyloid angiopathy; Aβ40WT, wild-type Aβ40 peptide; Aβ40DI, Dutch/Iowa cerebral amyloid angiopathy double mutant Aβ40 peptide; MBP, myelin basic protein; Aβ42WT, wild-type Aβ42 peptide; PBS, phosphate-buffered saline; BSA, bovine serum albumin; SDS−PAGE, sodium dodecyl sulfate−polyacrylamide gel electrophoresis; CD, circular dichroism; SPR, surface plasmon resonance; ECP, eosinophil cationic protein; ATR, attenuated total reflectance; TEM, transmission electron microscopy; AFM, atomic force microscopy; mAb, monoclonal antibody.

 Published on Web 04/22/2009

MATERIALS AND METHODS

Reagents and Chemicals. Aβ42 and Aβ40 peptides were synthesized by solid phase Fmoc (9-fluorenylmethoxycarbonyl) amino acid chemistry, purified by reverse phase high-performance liquid chromatography, and structurally characterized as previously described (*26*). N-Terminally biotinylated Aβ42 peptide was purchased from American Peptide Co. (Sunnyvale, CA). Scrambled Aβ42 peptide was purchased from AnaSpec (San Jose, CA). Eosinophil cationic protein (ECP) was purchased from Innovative Research (Novi, MI). Aβ42 peptides were initially prepared in hexafluoroisopropanol, lyophilized, and resuspended in either dimethyl sulfoxide (Me_2SO) or 100 mM NaOH as previously described (*27*). Purified human MBP (purchased from Chemicon International, Temecula, CA) was resuspended in 20 mM sodium acetate and 100 mM sodium chloride (pH 4.0), dialyzed into phosphate-buffered saline (PBS), and stored at −70 °C at 1 mg/mL. Purified bovine lactalbumin and thioflavin T were purchased from Sigma-Aldrich (St. Louis, MO). Anti-Aβ mAb 3D6 was generously provided by Lilly Research Laboratories (Indianapolis, IN). Anti-MBP antibodies mouse mAb 384, mouse mAb 382, and rabbit pAb 980 were purchased from Chemicon International. Biotinylation of mAbs was carried out using EZ-Link Sulfo-NHS-LC-LC-biotin (Pierce, Rockford, IL) according to the manufacturer's instructions.

Co-Immunoprecipitation Experiments. Aβ42 peptides were resuspended in Me_2SO to 2.5 mM and used at 10.8 μM. Purified MBP was used at 1.56 μM. Proteins were combined in 250 μL of incubation buffer (PBS/0.05% Tween 20/1% BSA). Anti-MBP mAb 382 was added to each sample mixture and each mixture incubated for 1 h at 4 °C with rocking. After incubation, 20 μL of washed GammaBind protein G Sepharose beads (Amersham) was added to each mixture, each of which was then incubated for an additional 1 h at 4 °C with rocking.

For competitive co-immunoprecipitation experiments, MBP was first immobilized to GammaBind beads at 1 μg of MBP per 80 μL of beads using mAb 382 and incubated for 1 h at 4 °C in incubation buffer. Biotinylated Aβ42WT peptide was resuspended in Me_2SO to 2.5 mM and used at 12.5 μM. Aβ40WT and scrambled A42WT were resuspended in Me_2SO to 2.5 mM and used at 125 μM. Proteins were combined with 20 μL of washed MBP-immobilized beads and incubated for 1 h at 4 °C with rocking.

For co-immunoprecipitations from brain homogenates, ~200 μg of brain cortical tissue from either human AD brain or one-year-old 5xFAD mice (*28*) was homogenized in 50 mM Tris (pH 7.4) and 200 mM NaCl with Complete Protease Inhibitor (Roche) on ice. Aliquots received either approximately 400 μg of anti-MBP polyclonal IgG or no antibody as a control. Aliquots were then incubated with 20 μL of GammaBind protein G Sepharose beads for 1 h at 4 °C with rocking.

After all the incubations described above, the beads were separated by centrifugation at 8000*g* for 2 min. Supernatants were removed, and beads were washed with 1 mL of incubation buffer. Separation and washing were repeated three times. A final wash was performed in a PBS/0.05% Tween 20 mixture to remove excess BSA. Centrifuged beads were combined with 25 μL of reducing SDS−PAGE sample loading buffer and heated. Ten microliters of each sample/loading buffer mix was loaded onto 10−20% Tricine gels (Invitrogen) and electrophoresed at 125 V for 90 min. Gels were transferred to Hybond ECL nitrocellulose membranes (Amersham Biosciences) at 50 V overnight at 4 °C. Membranes were blocked in PBS containing 5% bovine serum albumin (BSA) at room temperature for 1 h and washed 3 × 10 min with 5% BSA/PBS and 0.05% Tween 20. Membranes were incubated with primary antibodies for 1 h where applicable and washed as described above. Next, the membranes were incubated with horseradish peroxidase-conjugated streptavidin (Amersham Biosciences) for 1 h and washed. Detection was accomplished using ECL Western blotting substrate (Pierce). Experiments were performed in triplicate.

Surface Plasmon Resonance. All runs were performed on a BiaCore 2000 instrument (BiaCore, Uppsala, Sweden) with 10 mM HEPES (pH 7.4), 150 mM NaCl, 3 mM EDTA, and 0.005% (v/v) Tween 20 as running buffer and diluent. N-Terminally biotinylated Aβ42 peptides were resuspended in Me_2SO to 2.5 mM and serially diluted to 13 nM immediately before application. Aβ42 was bound to flow cell 2 at 10 μL/min to achieve an average relative response level of 157.1 RU leaving flow cell 1 as a reference. This chip preparation procedure was found to result in a surface that minimized mass transfer effects for kinetic interaction studies. The resultant R_{max} of this surface was approximately 700 RU with both MBP and ECP as the analyte. Purified MBP was passed over both flow cells at 6.25, 12.5, 25, 50, and 100 nM, while ECP was run at 0.2, 0.4, 0.8, 1.6, and 3.2 μM in triplicate at flow rates of 30 μL/min for kinetic measurements. Faster flow rates did not significantly improve the quality of data. Surfaces were regenerated with 0.2 M glycine (pH 2.0) and 150 mM NaCl between runs. The resulting sensorgrams were analyzed with BiaCore Analysis.

Circular Dichroism Spectroscopy. Lyophilized Aβ42 peptides were first resuspended with 100 mM NaOH to 2.4 mM, diluted to 50 μM in 10 mM potassium phosphate (pH 8.0) and 11 mM NaCl, and then incubated at 37 °C either alone or with 6.25 μM MBP. CD measurements from 190 to 260 nm were taken using an Olis RSM 1000 CD spectrophotometer (Online Instrument Systems, Bogart, GA). Six scans using adaptive acquisition timing were averaged for each sample using Olis software. The 1 mm quartz cuvettes used for sample data collection were cleaned between readings using 6 N HCl followed by a methanol rinse.

Attenuated Total Reflection Infrared Spectroscopy. Lyophilized Aβ42 peptides were first resuspended with 100 mM NaOH to 2.4 mM, diluted to 50 μM in PBS, and then incubated at 37 °C either alone or with 6.25 μM MBP. At the required time points, 100 μg of protein was dried onto an ATR plate and scanned using a Bruker IFS 66v/S infrared spectrometer. Spectra were recorded using 2000 scans over the range of 4000−400 cm^{-1}.

Thioflavin T Fluorescence Assay. Lyophilized Aβ42 peptides were first resuspended with Me_2SO to 2.5 mM, diluted to 12.5 μM in PBS, and then incubated at 37 °C with rocking either alone, with 1.56 μM MBP, or with 1.56 μM bovine lactalbumin. Control samples containing 0.5% Me_2SO and 1.56 μM MBP or 1.56 μM lactalbumin in PBS were also included. At each time point, 100 μL samples of each reaction were placed in a 96-well microplate in triplicate and 5 μL of 100 μM thioflavin T was added. The plate was mixed and incubated at 22 °C in the dark for 10 min. Fluorescence was measured at 490 nm using an excitation wavelength of 446 nm in a SpectraMax spectrofluorimeter (Molecular Devices, Sunnyvale, CA) using SoftMax Pro control software.

Transmission Electron Microscopy. Sample mixtures were deposited onto carbon-coated copper mesh grids (EM Sciences, Hatfield, PA) and negatively stained with 2% (w/v) uranyl acetate. The samples were viewed with a FEI Tecnai 12 BioTwin transmission electron microscope, and digital images were taken with an AMT camera.

Atomic Force Microscopy. AFM was conducted using a LifeScan controller developed by LifeAFM (Port Jefferson, NY) interfaced with a Digital Instruments (Santa Barbara, CA) MultiMode microscope fitted with an E scanner. AFM samples were first titrated to pH 4 using dilute HCl and then adsorbed onto freshly cleaved ruby mica (S&J Trading, Glen Oaks, NY). The lower pH allows for better adsorption of Aβ42 peptides to the negatively charged mica surface. Samples were imaged under hydrated conditions using supersharp silicon probes (SSS-Cont, Nanosensors, Neuchatel, Switzerland) that were modified for magnetic retraction by attaching samarium cobalt particles (LifeAFM). We estimate the effective diameter of the supersharp silicon probes to be 4 ± 1 nm at a height of 2 nm. Data analysis and creation of graphics were performed using Interactive Display Language 5.0 (Research Systems Inc., Boulder, CO). In the *Z* scale bars, numbers in each color square indicate the *Z* value at the middle of the range for that color.

RESULTS

MBP Interacts with Fibrillogenic Aβ42 Peptide. Previously, we reported the interaction of MBP with a familial CAA mutant Aβ40 peptide containing E22Q (Dutch) and D23N (Iowa) mutations (Aβ40DI) (*25*). It was also shown that MBP could bind the Aβ40WT peptide, but with significantly less affinity. Here, we demonstrate using co-immunoprecipitation that MBP also interacts with the longer, more fibrillogenic, Aβ42WT peptide. Samples containing MBP alone, MBP and Aβ42WT, or Aβ42WT alone were incubated with anti-MBP mAb 382 and precipitated with protein G-coated beads (Figure 1A). Duplicate immunoblot analyses were performed on each sample with either biotinylated anti-MBP mAb 384 or biotinylated anti-Aβ mAb 3D6. Aβ42WT was precipitated only in the presence of MBP and was not pulled down in the absence of MBP. The specificity of the interaction between Aβ42WT and MBP in this assay was examined by competition with an excess of Aβ40WT and a scrambled Aβ42WT peptide. Aβ42WT was inhibited from binding to MBP only in the presence of excess Aβ40WT and not in the presence of the scrambled Aβ42WT peptide, indicating that the interaction is specific (Figure 1B). Densitometric analysis of the immunoblots from the competitive co-immunoprecipitation studies showed that excess Aβ40WT inhibited the binding of Aβ42WT to MBP by approximately 85% (Figure 1C).

Aβ was immunoprecipitated from soluble cortical homogenates prepared from both human AD brain and 5xFAD mouse brain. These data indicate that MBP can interact with Aβ peptides at a sufficient strength to associate in the presence of a complex mixture of biomolecules in brain homogenate.

To more quantitatively analyze the affinity between MBP and Aβ42, we next performed SPR measurements. Aβ42WT peptide ligand surfaces and other assay parameters were designed as described in Materials and Methods. Increasing concentrations of MBP were passed over the ligand surface, and the resultant sensorgrams were analyzed using BIAanalysis. From this, the kinetics of the interactions were determined (Table 1). The

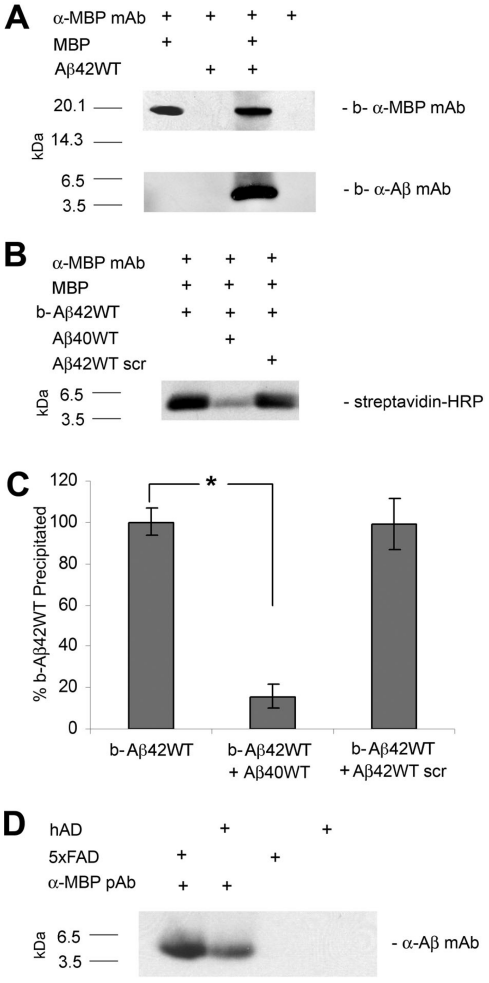

FIGURE 1: Co-immunoprecipitation of MBP and Aβ42WT. (A) The Aβ42WT peptide was co-immunoprecipitated with MBP using anti-MBP mAb 382 as described in Materials and Methods. Immunoprecipitated samples from left to right were as follows: MBP alone, Aβ42WT alone, MBP incubated with Aβ42WT, negative control (no MBP and no Aβ42WT). (B) Representative immuoblot showing the co-immunoprecipitation of biotinylated Aβ42WT with MBP was effectively competed with excess Aβ40WT peptide but not excess scrambled Aβ42WT peptide. (C) Quantitation of the competitive co-immunoprecipitation assays. The data presented are means ± the standard deviation of triplicate experiments (*$p < 0.001$). (D) Immunoprecipitation from soluble cortical brain homogenates of human AD brain and 5xFAD mouse brain using polyclonal anti-MBP IgG. Immunoprecipitations from left to right are as follows: 5xFAD mouse brain, human AD brain, 5xFAD control, and human AD control.

calculated K_D between MBP and Aβ42WT is comparable to the affinity between MBP and Aβ40DI and is stronger than that between MBP and Aβ40WT as reported previously (*25*). Eosinophil cationic protein (ECP), which has a charge and a molecular mass very similar to those of MBP, was used as a negative control to test the specificity of the MBP−Aβ42WT interaction with SPR. No binding could be detected between the Aβ42WT ligand surface and ECP at concentrations up to 32-fold greater than that of MBP. Furthermore, ECP did not compete for MBP binding to Aβ42 in co-immunoprecipitation experiments (data not shown).

MBP Prevents the Formation of β-Sheet Structures in Aβ42WT in Vitro. After demonstrating the affinity between Aβ42WT and MBP in vitro, we next determined if this interaction could inhibit Aβ42WT fibrillogenesis. The assembly of fibrils

Table 1: Binding Affinities (K_D) of MBP and ECP for Aβ Peptides

	[MBP] (M)	[ECP] (M)
Aβ40DI	$(1.69 \pm 0.14) \times 10^{-8}$	not detected
Aβ42WT	$(4.29 \pm 0.28) \times 10^{-8}$	not detected
Aβ40WT	$(1.16 \pm 0.12) \times 10^{-7}$	not detected

from Aβ monomers is accompanied by the formation of β-sheet secondary structure within and between individual monomers (*29*). Therefore, we sought to examine the effect of MBP on the secondary structure of Aβ42WT using circular dichroism spectroscopy during fibrillogenesis.

First, we measured the time-dependent CD spectra between 190 and 260 nm for Aβ42WT, making scans at regular intervals from 0 to 36 h (Figure 2A). At 0 h, the Aβ42WT CD spectra displayed a characteristic negative peak at 197 nm, which correlates with the presence of abundant random-coil conformation. Over the course of 36 h, Aβ42WT adopts a predominantly β-sheet conformation as shown by the emergence of a characteristic positive peak at 195 nm and a negative peak at 215 nm. Similar incubations were also performed on Aβ42WT with MBP, as well as with MBP alone. Throughout the time course, MBP exhibited a characteristic random-coil conformation (data not shown) which has been previously reported (*30*).

It has been shown that plotting the absolute value of the CD signal at 215 nm versus time produces a curve indicative of the formation of β-sheet fibrils over time for Aβ peptides (*31*). In Figure 2B, the absolute values of the CD ellipticity for both MBP alone and Aβ42WT with MBP were compared to that of Aβ42WT alone. These data illustrate that Aβ42WT β-sheet formation proceeds linearly until 24 h where it begins to plateau. Conversely, for both MBP alone and Aβ42WT with MBP, the amplitude of the signal remained low and decreased somewhat over the course of incubation, suggesting a lack of β-sheet formation. At 48 h, a sample of Aβ42WT, which demonstrated a high abundance of β-sheet, was spiked with MBP and scanned immediately (Figure 2C). This was compared to a scan at 48 h of Aβ42WT with MBP to illustrate the difference between a sample containing MBP in the presence of β-sheet structure and a sample containing MBP without β-sheet structure. These data suggest that MBP is able to inhibit the formation of β-sheet structures from unstructured Aβ42WT monomers.

Attenuated total reflection (ATR) infrared spectroscopy was used to further examine the secondary structure of Aβ42WT in the presence of MBP. The IR spectra of a protein, especially absorbance in the amide I band ($\sim$1700−1600 cm^{-1}), are sensitive to changes in secondary structure (*32*−*34*). Spectra obtained for Aβ42WT incubated at 37 °C for 24 h had a main peak at 1635 cm^{-1} with a smaller shoulder peak at 1616 cm^{-1} which were assigned to major β-sheet structure. The peak at 1673 cm^{-1} is due to β-turn structure. When Aβ42WT was incubated in the presence of MBP, we measured two unresolved peaks at 1670 and 1648 cm^{-1} assigned to β-turn and α-helical/unordered structures, respectively (Figure 3A). The contributing peaks in the amide I band, however, are overlapping and convoluted, making interpretation of secondary structure difficult in many cases as it is with these data. By plotting the second derivative of the spectra, we can resolve the contributing components and study their relative contribution (*32*). When the data are plotted in this manner, it shows that both Aβ42WT alone and Aβ42WT with MBP contain identical peaks at 1681 and

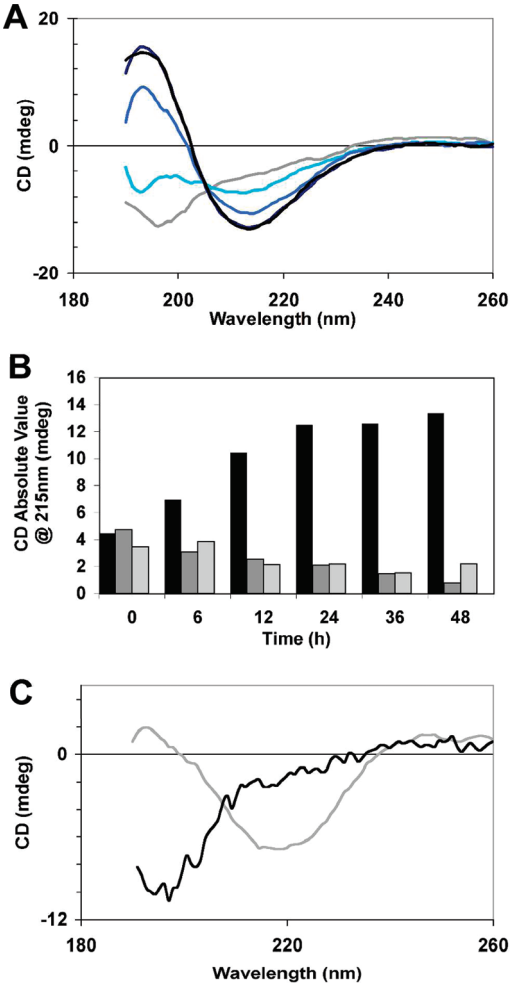

FIGURE 2: Inhibition of Aβ42WT β-sheet formation by MBP, assessed by CD spectroscopy. Peptides were prepared and scanned as described in Materials and Methods. (A) Successive scans of Aβ42WT incubated at 37 °C taken at 0 (gray), 6 (teal), 12 (light blue), 24 (dark blue), and 36 h (black). (B) Absolute values at 215 nm charted from successive scans of Aβ42 (black), MBP (dark gray), and Aβ42 with MBP (light gray). (C) Single scan of Aβ42WT with MBP at 48 h (black) compared to a single scan of mature Aβ42WT fibrils spiked with MBP at 48 h (gray).

1675 cm^{-1} due to the presence of β-turn structure. Aβ42WT with MBP shows two peaks at 1658 and 1650 cm^{-1} assigned to α-helical and unstructured elements, respectively. Both samples with and without MBP have peaks at 1697 and 1616 cm^{-1} in the β-sheet regions; however, the contribution is higher in the Aβ42WT sample without MBP. Aβ42WT alone also shows a strong β-sheet contribution at 1633 cm^{-1} that is much larger than the peak at 1635 cm^{-1} for Aβ42WT with MBP. The signal at 1635 cm^{-1} also is more shifted away from β-sheet and toward the α-helical and unstructured region of the band and contains unresolved α-helical and unstructured elements as well in its shoulder (Figure 3B). This confirms the CD measurements that show less β-sheet structure in Aβ42WT in the presence of MBP.

This inhibitory effect was also confirmed by using a thioflavin T fluorescence assay. We found that an 8-fold lower molar concentration of MBP was sufficient to dramatically inhibit Aβ42WT fibril formation (Figure 4). No change in Aβ42WT thioflavin T fluorescence was seen when the experiment was performed in the presence of a similarly sized negative control protein (bovine lactalbumin) under these conditions.

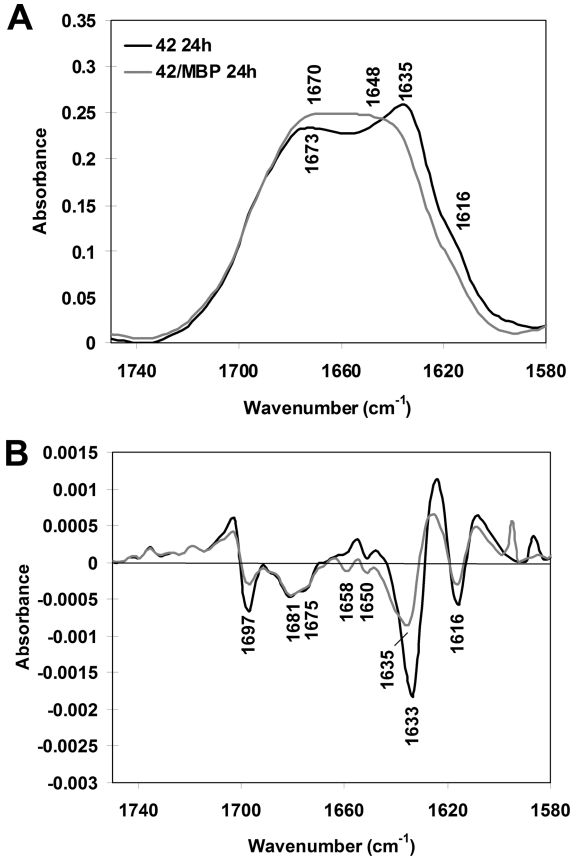

FIGURE 3: Inhibition of Aβ42WT β-sheet formation by MBP assessed by ATR-IR. Peptides were prepared and scanned as described in Materials and Methods. (A) IR absorbance in the amide I band for Aβ42WT alone (black line) or Aβ42WT with MBP (gray line) incubated at 37 °C for 24 h. (B) Second-derivative plot of IR spectra in panel A.

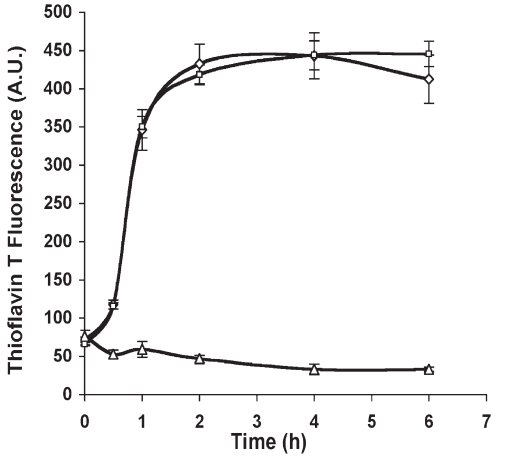

FIGURE 4: Thioflavin T analysis for inhibition of Aβ42WT fibril formation by MBP. Aβ42 was treated with HFIP, resuspended to a concentration of 2.5 mM in DMSO, and then diluted to a concentration of 12.5 μM in PBS in the absence (◇) or presence of 1.56 μM MBP (△) or 1.56 μM α-lactalbumin (□) as a control. At specific time points, aliquots were collected from each sample and subjected to thioflavin T binding and fluorescence to determine fibrillar assembly as described in Materials and Methods. The data shown are means ± the standard deviation of triplicate samples.

MBP Inhibits the Formation of Aβ42 Fibrils. The inhibition of fibril assembly was further confirmed by TEM and single-touch AFM analysis. After incubation for 6 h in the absence of MBP, oligomeric structures become evident (Figure 5). These oligomeric structures can reach lengths of up to 40 nm and heights of up to ~3.5 nm. By 24 h, these oligomeric structures had assembled into fibrillar structures measuring several hundred nanometers in length with an average height of more than 4 nm. In the presence of substoichiometric amounts of MBP, the extent of formation of these structures was greatly reduced, indicating an inhibition of fibril formation by MBP.

DISCUSSION

Aβ42WT is much more fibrillogenic than Aβ40WT and has been shown to form soluble and insoluble oligomeric forms different from those of Aβ40WT (*35*). Many of these Aβ42WT oligomeric assemblies have been shown to be more cytotoxic than Aβ40WT oligomeric assemblies (*36*−*38*) and to act as seeds for the formation of Aβ40WT fibrils (*9*). Aβ42WT levels in brain tissue have been shown to increase after head injury, possibly predisposing patients to AD-like symptoms (*39*). Mutations that result in a high likelihood of developing AD often result in an increase in Aβ42WT production (*40*). For these reasons, the role of Aβ42WT has increasingly come under scrutiny in the pathology of AD and related disorders.

Previously, we have demonstrated that MBP binds to and inhibits the fibrillogenesis of familial CAA mutant forms of Aβ as well as its weaker ability to bind to Aβ40WT (*25*). We hypothesized that this interaction may be a possible explanation for the regional differences seen in the deposition of fibrillar amyloid within the brains of patients and animal models with these familial CAA mutant forms of Aβ. Although we have begun to understand how MBP interacts with CAA mutant Aβ40, it was not known whether a similar interaction would take place with the more fibrillogenic Aβ42WT peptide.

In this study, we show that MBP can, in fact, bind to and inhibit the fibrillogenesis of the Aβ42WT peptide in vitro. Co-immunoprecipitation experiments (Figure 1) demonstrate that Aβ42WT interacts with MBP. This interaction was demonstrated to be specific by the failure of a scrambled Aβ42WT peptide to compete with Aβ42WT to bind with MBP and the competition of Aβ40WT with this binding to MBP (Figure 1B,C). Similarly, Aβ peptides were coprecipitated with MBP using a polyclonal antibody to MBP from cortical brain homogenates of human AD brain tissue or 5xFAD mouse brain, a transgenic mouse model that produces high levels of Aβ42WT in its brain tissue (*28*) (Figure 1D). Although it is not conclusive from these data alone whether MBP and Aβ normally associate in vivo, it does demonstrate that in the complex mixture of a brain homogenate the interaction between MBP and Aβ peptides is of sufficient specificity to facilitate coprecipitation.

Although Aβ42WT does not contain either the Dutch or the Iowa mutations, it is highly fibrillogenic, suggesting that the interaction does not require the mutant residues at positions 22 and 23, but rather that MBP may be interacting with a certain conformation common to both Aβ42WT and familial CAA mutant Aβ40DI. Consistent with this idea, affinity values for Aβ42WT and MBP were also higher than those obtained for Aβ40WT and MBP reported previously (*25*). Aβ40WT is much less fibrillogenic than Aβ42WT, lending weight to the hypothesis that MBP is interacting with conformations more prevalent in suspensions of more fibrillogenic Aβ peptides. Further study will be necessary to elucidate the precise nature of these interactions.

By using CD spectroscopy, we demonstrate that the interaction between MBP and Aβ42WT resulted in a reduction in the

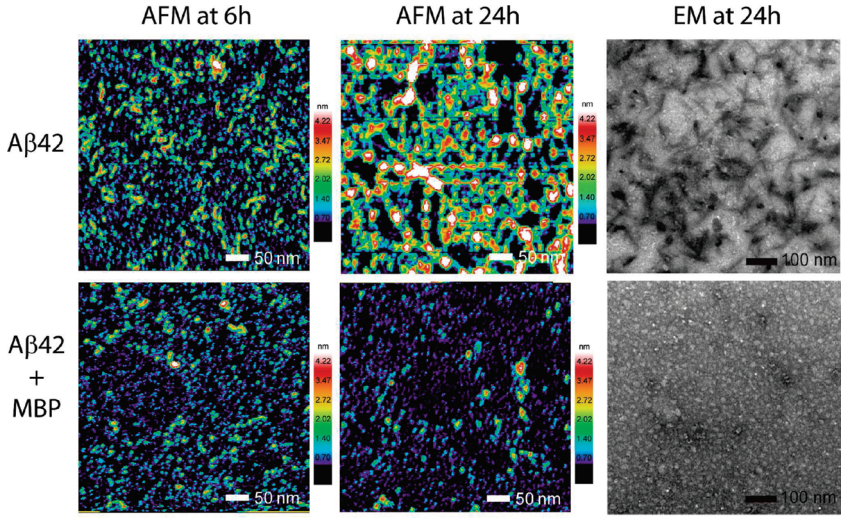

FIGURE 5: AFM and TEM images of the inhibition of Aβ42WT fibril formation by MBP. Aβ42WT samples were incubated at 37 °C in the absence (top row) or presence (bottom row) of MBP at the same Aβ42WT:MBP ratio used in the thioflavin T analysis. AFM images were scanned after incubation for 6 and 24 h. EM images were taken after incubation for 24 h.

adoption of β-sheet structure when compared to Aβ42WT alone (Figure 2). By plotting the absolute value at 215 nm for successive scans, we were able to quantitate the emergence of β-sheet structure in our samples over time (Figure 2B). We show that in the presence of MBP, which remains in a random coil conformation, Aβ42WT is unable to form appreciable β-sheet structures.

To determine whether this failure to detect a β-sheet signature was due to signal quenching by MBP present in the sample, we performed a scan on mature (48 h) Aβ42WT fibrils (as determined through CD analysis), which was spiked with MBP and immediately scanned. The signal obtained with this spiked control sample was compared to the signal obtained from a sample of Aβ42WT incubated for 48 h with MBP (Figure 2C). The spiked sample clearly showed the presence of β-sheet structures as evidenced by a negative peak at 215 nm. This was an indication that had the Aβ42WT peptides formed β-sheet secondary structures in the presence of MBP, they would have been detected.

Further evidence of the inhibition of β-sheet structures was obtained through second-derivative ATR-IR analysis. In the presence of MBP, the β-sheet contribution is much diminished though not completely extinguished, suggesting an inhibition of larger β-sheet oligomers (Figure 3B). The typical β-hairpin loop structure of Aβ42WT monomers contains antiparallel β-sheet structure which if left intact would explain the small β-sheet structural component seen in the spectra of samples containing MBP. Further, the peaks at 1681 and 1675 cm^{-1} which are attributed to β-turn structure remained unchanged even with the addition of MBP, suggesting that the β-hairpin structure of Aβ42WT is intact in the presence of MBP. These data suggest that MBP is interacting with Aβ42WT monomers in a manner that leaves their β-hairpin structure intact but inhibits the formation of larger β-sheet oligomers.

The inhibition of the formation of β-sheet oligomers and fibrils in Aβ42WT by MBP is supported by thioflavin T analysis, which demonstrates a lack of thioflavin T fluorescence in samples containing Aβ42WT and MBP (Figure 4). This observation further indicates an inhibition of fibril formation by MBP. The rate of fibril formation in the thioflavin T assay, when compared to the rate observed in the CD measurements, was much more rapid. A plateau in thioflavin T fluorescence was reached at approximately 2 h, while samples measured by CD reached a plateau only after 12 h. This difference can be explained by the difference in the NaCl concentrations used for these experiments. The NaCl concentration was 150 mM in samples used for thioflavin T measurements, while for CD spectroscopy, the NaCl concentration was 11 mM. A lower salt concentration was used for CD experiments because high salt concentrations interfere with CD measurements between 190 and 210 nm.

These results are further supported by direct visualization of amyloid fibril assembly using both TEM and AFM at longer time points (Figure 5). The formation of short oligomeric structures becomes evident at 6 h as detected by both AFM and TEM for Aβ42WT alone. However, when MBP is present, there appears to be a marked reduction in the levels of these structures. Upon continuous incubation of Aβ42WT for 24 h, larger fibrils are seen. By TEM, these fibrils appear to range between 50 and 200 nm in length and are noticeably absent when MBP is present.

Our results indicate that MBP can interact with Aβ42WT in vitro and inhibit its fibrillogenesis. Previous studies have shown that MBP can bind to and inhibit the fibrillogenesis of the CAA double mutant Aβ40DI peptide (*25*). At present, it is unknown if MBP interacts with both peptides in a similar manner.

It has been shown that different Aβ peptides may assemble along different or multiple folding pathways giving rise to heterogeneous mixtures of structures whose ratios may be unique from peptide to peptide. Given the likely differences between the folding pathways of Aβ40WT, Aβ42WT, and Aβ40DI and the fact that their affinity for MBP increases with rising fibrillization rate, it may be possible that a subset of conformations favored by the more fibrillogenic peptides are responsible for the bulk of the interaction with MBP. In other words, Aβ40WT suspensions may lack or have fewer of these specific conformations more common to Aβ42WT and Aβ40DI suspensions, explaining the lower affinity between MBP and Aβ40WT and the higher affinity with Aβ42WT and Aβ40DI. Further study will be necessary to elucidate the molecular basis for the interaction between MBP and Aβ peptides.

However, this interaction raises intriguing questions about the role MBP, or MBP-related peptides, may play in association with Aβ42WT and what role this interaction may play in the

pathogenesis of AD and other related disorders. For instance, MBP may serve to suppress the deposition and seeding of amyloid plaques at their earliest stages of formation. Alterations in levels of intact MBP or derived fragments may affect how Aβ peptides are retained or cleared from brain. It may also be possible that although MBP inhibits the formation of fibrils it may stabilize the formation of neurotoxic oligomers and thereby exacerbate disease pathology.

It is interesting to note that deposits of Aβ found in regions of white matter, which are rich in myelinated axons, are often diffuse and nonfibrillar (*41*, *42*). Damage to white matter is known to result in an increase in the level of myelin proteins and especially MBP-related peptides in the cerebral spinal fluid (*43*). Microglia have also been shown to secrete GOLLI-MBP proteins when activated (*44*, *45*). This release of MBP into the extracellular environment in AD patients with white matter damage and/or activated microglia could provide ample opportunities for this interaction with Aβ to take place and inhibit the formation of fibrils, though further in vivo study will be needed to confirm this. These findings point to the need to improve our understanding of the effect of changes in white matter as well as the role of MBP-related peptides in the brain and how they relate to AD progression.

REFERENCES

1. Selkoe, D. J. (2001) Alzheimer's disease: Genes, proteins, and therapy. *Physiol. Rev. 81*, 741–766.
2. Kang, J., Lemaire, H. G., Unterbeck, A., Salbaum, J. M., Masters, C. L., Grzeschik, K. H., Multhaup, G., Beyreuther, K., and Muller-Hill, B. (1987) The precursor of Alzheimer's disease amyloid A4 protein resembles a cell-surface receptor. *Nature 325*, 733–736.
3. Goldgaber, D., Lerman, M. I., McBride, O. W., Saffiotti, U., and Gajdusek, D. C. (1987) Characterization and chromosomal localization of a cDNA encoding brain amyloid of Alzheimer's disease. *Science 235*, 877–880.
4. Tanzi, R. E., Gusella, J. F., Watkins, P. C., Bruns, G. A., St George-Hyslop, P., Van Keuren, M. L., Patterson, D., Pagan, S., Kurnit, D. M., and Neve, R. L. (1987) Amyloid β protein gene: cDNA, mRNA distribution, and genetic linkage near the Alzheimer locus. *Science 235*, 880–884.
5. Robakis, N. K., Ramakrishna, N., Wolfe, G., and Wisniewski, H. M. (1987) Molecular cloning and characterization of a cDNA encoding the cerebrovascular and the neuritic plaque amyloid peptides. *Proc. Natl. Acad. Sci. U.S.A. 84*, 4190–4194.
6. Roher, A. E., Lowenson, J. D., Clarke, S., Woods, A. S., Cotter, R. J., Gowing, E., and Ball, M. J. (1993) β-Amyloid-(1−42) is a major component of cerebrovascular amyloid deposits: Implications for the pathology of Alzheimer disease. *Proc. Natl. Acad. Sci. U.S.A. 90*, 10836–10840.
7. Masters, C. L., Simms, G., Weinman, N. A., Multhaup, G., McDonald, B. L., and Beyreuther, K. (1985) Amyloid plaque core protein in Alzheimer disease and Down syndrome. *Proc. Natl. Acad. Sci. U.S.A. 82*, 4245–4249.
8. Dolev, I., and Michaelson, D. M. (2006) The nucleation growth and reversibility of Amyloid-β deposition in vivo. *J. Alzheimer's Dis. 10*, 291–301.
9. McGowan, E., Pickford, F., Kim, J., Onstead, L., Eriksen, J., Yu, C., Skipper, L., Murphy, M. P., Beard, J., Das, P., Jansen, K., Delucia, M., Lin, W. L., Dolios, G., Wang, R., Eckman, C. B., Dickson, D. W., Hutton, M., Hardy, J., and Golde, T. (2005) Aβ42 is essential for parenchymal and vascular amyloid deposition in mice. *Neuron 47*, 191–199.
10. Findeis, M. A. (2007) The role of amyloid β peptide 42 in Alzheimer's disease. *Pharmacol. Ther. 116*, 266–286.
11. Vinters, H. V. (1987) Cerebral amyloid angiopathy. A critical review. *Stroke 18*, 311–324.
12. Jellinger, K. A. (2002) Alzheimer disease and cerebrovascular pathology: An update. *J. Neural Transm. 109*, 813–836.
13. Thal, D. R., Ghebremedhin, E., Orantes, M., and Wiestler, O. D. (2003) Vascular pathology in Alzheimer disease: Correlation of cerebral amyloid angiopathy and arteriosclerosis/lipohyalinosis with cognitive decline. *J. Neuropathol. Exp. Neurol. 62*, 1287–1301.
14. Levy, E., Carman, M. D., Fernandez-Madrid, I. J., Power, M. D., Lieberburg, I., van Duinen, S. G., Bots, G. T., Luyendijk, W., and Frangione, B. (1990) Mutation of the Alzheimer's disease amyloid gene in hereditary cerebral hemorrhage, Dutch type. *Science 248*, 1124–1126.
15. Van Broeckhoven, C., Haan, J., Bakker, E., Hardy, J. A., Van Hul, W., Wehnert, A., Vegter-Van der Vlis, M., and Roos, R. A. (1990) Amyloid β protein precursor gene and hereditary cerebral hemorrhage with amyloidosis (Dutch). *Science 248*, 1120–1122.
16. Hendriks, L., van Duijn, C. M., Cras, P., Cruts, M., Van Hul, W., van Harskamp, F., Warren, A., McInnis, M. G., Antonarakis, S. E., and Martin, J. J.; et al. (1992) Presenile dementia and cerebral haemorrhage linked to a mutation at codon 692 of the β-amyloid precursor protein gene. *Nat. Genet. 1*, 218–221.
17. Kamino, K., Orr, H. T., Payami, H., Wijsman, E. M., Alonso, M. E., Pulst, S. M., Anderson, L., O'Dahl, S., Nemens, E., and White, J. A.; et al. (1992) Linkage and mutational analysis of familial Alzheimer disease kindreds for the APP gene region. *Am. J. Hum. Genet. 51*, 998–1014.
18. Tagliavini, F., Rossi, G., Padovani, A., Magoni, M., Andora, G., Sgarzi, M., Bizzi, A., Savioardo, M., Carella, F., Morbin, M., Giaccone, G., and Bugiani, O. (1999) A new APP mutation related to hereditary cerebral hemorrhage. *Alzheimer's Rep. 2*, S28.
19. Grabowski, T. J., Cho, H. S., Vonsattel, J. P., Rebeck, G. W., and Greenberg, S. M. (2001) Novel amyloid precursor protein mutation in an Iowa family with dementia and severe cerebral amyloid angiopathy. *Ann. Neurol. 49*, 697–705.
20. Davis, J., and Van Nostrand, W. E. (1996) Enhanced pathologic properties of Dutch-type mutant amyloid β-protein. *Proc. Natl. Acad. Sci. U.S.A. 93*, 2996–3000.
21. Verbeek, M. M., de Waal, R. M., Schipper, J. J., and Van Nostrand, W. E. (1997) Rapid degeneration of cultured human brain pericytes by amyloid β protein. *J. Neurochem. 68*, 1135–1141.
22. Miravalle, L., Tokuda, T., Chiarle, R., Giaccone, G., Bugiani, O., Tagliavini, F., Frangione, B., and Ghiso, J. (2000) Substitutions at codon 22 of Alzheimer's Aβ peptide induce diverse conformational changes and apoptotic effects in human cerebral endothelial cells. *J. Biol. Chem. 275*, 27110–27116.
23. Melchor, J. P., McVoy, L., and Van Nostrand, W. E. (2000) Charge alterations of E22 enhance the pathogenic properties of the amyloid β-protein. *J. Neurochem. 74*, 2209–2212.
24. Van Nostrand, W. E., Melchor, J. P., Cho, H. S., Greenberg, S. M., and Rebeck, G. W. (2001) Pathogenic effects of D23N Iowa mutant amyloid β-protein. *J. Biol. Chem. 276*, 32860–32866.
25. Hoos, M. D., Ahmed, M., Smith, S. O., and Van Nostrand, W. E. (2007) Inhibition of familial cerebral amyloid angiopathy mutant amyloid β-protein fibril assembly by myelin basic protein. *J. Biol. Chem. 282*, 9952–9961.
26. Burdick, D., Soreghan, B., Kwon, M., Kosmoski, J., Knauer, M., Henschen, A., Yates, J., Cotman, C., and Glabe, C. (1992) Assembly and aggregation properties of synthetic Alzheimer's A4/β amyloid peptide analogs. *J. Biol. Chem. 267*, 546–554.
27. Stine, W. B.Jr., Dahlgren, K. N., Krafft, G. A., and LaDu, M. J. (2003) In vitro characterization of conditions for amyloid-β peptide oligomerization and fibrillogenesis. *J. Biol. Chem. 278*, 11612–11622.
28. Oakley, H., Cole, S. L., Logan, S., Maus, E., Shao, P., Craft, J., Guillozet-Bongaarts, A., Ohno, M., Disterhoft, J., Van Eldik, L., Berry, R., and Vassar, R. (2006) Intraneuronal β-amyloid aggregates, neurodegeneration, and neuron loss in transgenic mice with five familial Alzheimer's disease mutations: Potential factors in amyloid plaque formation. *J. Neurosci. 26*, 10129–10140.
29. Nelson, R., and Eisenberg, D. (2006) Recent atomic models of amyloid fibril structure. *Curr. Opin. Struct. Biol. 16*, 260–265.
30. Harauz, G., Ishiyama, N., Hill, C. M., Bates, I. R., Libich, D. S., and Fares, C. (2004) Myelin basic protein-diverse conformational states of an intrinsically unstructured protein and its roles in myelin assembly and multiple sclerosis. *Micron 35*, 503–542.
31. Bartolini, M., Bertucci, C., Bolognesi, M. L., Cavalli, A., Melchiorre, C., and Andrisano, V. (2007) Insight into the kinetic of amyloid β (1−42) peptide self-aggregation: Elucidation of inhibitors' mechanism of action. *ChemBioChem 8*, 2152–2161.
32. Susi, H., and Byler, D. M. (1983) Protein structure by Fourier transform infrared spectroscopy: Second derivative spectra. *Biochem. Biophys. Res. Commun. 115*, 391–397.
33. Haris, P. I., and Chapman, D. (1994) Analysis of polypeptide and protein structures using Fourier transform infrared spectroscopy. *Methods Mol. Biol. 22*, 183–202.
34. Jackson, M., and Mantsch, H. H. (1995) The use and misuse of FTIR spectroscopy in the determination of protein structure. *Crit. Rev. Biochem. Mol. Biol. 30*, 95–120.

35. Bitan, G., Kirkitadze, M. D., Lomakin, A., Vollers, S. S., Benedek, G. B., and Teplow, D. B. (2003) Amyloid β-protein (Aβ) assembly: Aβ40 and Aβ42 oligomerize through distinct pathways. *Proc. Natl. Acad. Sci. U.S.A. 100*, 330–335.
36. Hoshi, M., Sato, M., Matsumoto, S., Noguchi, A., Yasutake, K., Yoshida, N., and Sato, K. (2003) Spherical aggregates of β-amyloid (amylospheroid) show high neurotoxicity and activate τ protein kinase I/glycogen synthase kinase-3β. *Proc. Natl. Acad. Sci. U.S.A. 100*, 6370–6375.
37. Walsh, D. M., and Selkoe, D. J. (2007) Aβ oliogmers: A decade of discovery. *J. Neurochem. 101*, 1172–1184.
38. Haass, C., and Selkoe, D. J. (2007) Soluble protein oligomers in neurodegeneration: Lessons from the Alzheimer's amyloid β peptide. *Nat. Rev. Mol. Cell Biol. 8*, 101–112.
39. DeKosky, S. T., Abrahamson, E. E., Ciallella, J. R., Paljug, W. R., Wisniewski, S. R., Clark, R. S., and Ikonomovic, M. D. (2007) Association of increased cortical soluble Aβ42 levels with diffuse plaques after severe brain injury in humans. *Arch. Neurol. 64*, 541–544.
40. Borchelt, D. R., Thinakaran, G., Eckman, C. B., Lee, M. K., Davenport, F., Ratovitsky, T., Prada, C. M., Kim, G., Seekins, S., Yager, D., Slunt, H. H., Wang, R., Seeger, M., Levey, A. I., Gandy, S. E., Copeland, N. G., Jenkins, N. A., Price, D. L., Younkin, S. G., and Sisodia, S. S. (1996) Familial Alzheimer's disease-linked presenilin 1 variants elevate Aβ1−42/1−40 ratio in vitro and in vivo. *Neuron 17*, 1005–1013.
41. Behrouz, N., Defossez, A., Delacourte, A., and Mazzuca, M. (1991) The immunohistochemical evidence of amyloid diffuse deposits as a pathological hallmark in Alzheimer's disease. *J. Gerontol. 46*, B209–B212.
42. Wisniewski, H. M., Bancher, C., Barcikowska, M., Wen, G. Y., and Currie, J. (1989) Spectrum of morphological appearance of amyloid deposits in Alzheimer's disease. *Acta Neuropathol. 78*, 337–347.
43. Whitaker, J. N. (1998) Myelin basic protein in cerebrospinal fluid and other body fluids. *Mult. Scler. 4*, 16–21.
44. Papenfuss, T. L., Thrash, J. C., Danielson, P. E., Foye, P. E., Hllbrush, B. S., Sutcliffe, J. G., Whitacre, C. C., and Carson, M. J. (2007) Induction of Golli-MBP expression in CNS macrophages during acute LPS-induced CNS inflammation and experimental autoimmune encephalomyelitis (EAE). *ScientificWorldJournal 7*, 112–120.
45. Filipovic, R., and Zecevic, N. (2005) Lipopolysaccharide affects Golli expression and promotes proliferation of oligodendrocyte progenitors. *Glia 49*, 457–466.